

## Use of functionalized WS<sub>2</sub> nanotubes to produce new polystyrene/polymethylmethacrylate nanocomposites

W. Zhang<sup>a</sup>, S. Ge<sup>a</sup>, Y. Wang<sup>a</sup>, M.H. Rafailovich<sup>a</sup>, O. Dhez<sup>b</sup>, D.A. Winesett<sup>b</sup>, H. Ade<sup>b</sup>,  
Kurikka V.P.M. Shafi<sup>c</sup>, A. Ulman<sup>c</sup>, R. Popovitz-Biro<sup>d</sup>, R. Tenne<sup>d</sup>, J. Sokolov<sup>d,\*,1</sup>

<sup>a</sup>Department of Materials Science and Engineering, State University of New York at Stony Brook, Stony Brook, NY 11794, USA

<sup>b</sup>Department of Physics, North Carolina State University, Raleigh, NC 27695, USA

<sup>c</sup>Department of Chemistry and Chemical Engineering, Polytechnic University, 6 Metrotech Center, Brooklyn, NY 11230, USA

<sup>d</sup>Department of Materials and Interfaces, Weizmann Institute, Rehovot 76100, Israel

Received 31 July 2002; received in revised form 7 January 2003; accepted 9 January 2003

### Abstract

Multiwall WS<sub>2</sub> nanotubes of 40–50 nm diameter were functionalized with *n*-octadecyl phosphonic acid by sonication in toluene and blended with mixtures of polystyrene (PS) and polymethylmethacrylate (PMMA) to form new nanocomposite (NC) materials. The surface and domain structures were studied by atomic force microscopy (AFM), scanning transmission X-ray microscopy (STXM) and transmission electron microscopy (TEM) for various levels of loading of nanotubes up to 20 wt%. Phase-separated domain size and surface roughness of the nanocomposite films were found to be dramatically reduced relative to the pure homopolymer blend and good dispersal of the nanotubes in the blend matrix was attained.

© 2003 Published by Elsevier Science Ltd.

**Keywords:** Polymer composite materials; Polymer physics; Pure homopolymer blend

### 1. Introduction

Most combinations of long-chain polymers do not mix well and various strategies using copolymers (block or random), particulate fillers or chemical compatibilizers added to blends have been tried in order to promote mixing [1]. Fillers are widely used in industry in products such as tires, construction materials and airplanes [2] with the purpose of tailoring physical/mechanical properties and/or to reduce cost. The main variables, which control the nature of the composites, are particle size and shape, concentration and particle–matrix (polymer) chemical interactions. Typically, fillers are added at the level of 5–30% (by volume) with particle sizes commonly ranging from about 0.1 μm to tens of microns. Viscosity and dynamic elastic moduli,  $G'(\omega)$  and  $G''(\omega)$ , are observed to increase by large amounts in the range of one to three orders of magnitude [3], with

smaller particles having a larger effect for a give filler volume fraction. This is believed to be due to the increased volume of material ‘immobilized’ by contact with the filler. The increase in  $G'(\omega)$  and  $G''(\omega)$  is observed to be largest at low frequencies and has been attributed to the formation of networks of agglomerations [1] in the filler-matrix system. At higher frequencies, these networks are believed to break up and moduli approach values characteristic of the unfilled matrix. Properties of the filled materials may be further modified by surface treatment of the fillers with various coatings or coupling agents. Suetsugu and White [4] studied the mechanical properties of polystyrene (PS) containing spherical CaCO<sub>3</sub> particles, both with and without a stearic acid coating. Increases of viscosity by factors up to 200 were measured, and values up to  $4 \times 10^4$  Pa were found to be induced by the presence of fillers. The stearic acid coating acted to reduce particle–particle interactions, and hence agglomeration, and the changes in viscosity and yield values were decreased significantly. Also, phase separation kinetics and equilibrium phase diagrams of filled blends have been studied as a function of filler type and surface treatment [5].

\* Corresponding author. Present address: State University of New York at Stony Brook, NY, USA. Tel.: +1-631-632-8483; fax: +1-631-632-5764.

E-mail address: jsokolov@ms.cc.sunysb.edu (J. Sokolov).

<sup>1</sup> On leave from the State University of New York at Stony Brook.

In this study, we report an initial investigation of the properties of an immiscible polymer blend system, polystyrene/polymethylmethacrylate (PS/PMMA), modified by the addition of WS<sub>2</sub> nanotubes [6–8] as compatibilizer/fillers. The discovery of carbon nanotubes [9] and the realization that many layered semiconductor compounds can also be used to synthesize a wide variety of inorganic fullerenes and nanotubes [6] has led to the preparation of a wide variety of new materials with unusual physical properties. Several recent studies have been done on the incorporation of carbon nanotubes into homopolymer matrices [10–15], focusing on the dispersion, morphology and mechanical properties of the resulting composites. The main challenges are to find an effective method for dispersing nanotubes in the matrix and to produce a strong nanotube–matrix bond. The procedures used so far include (1) surface treatments to achieve suspensions in solution, followed by casting [10,14], (2) sonication of nanotube–polymer–solvent solutions and casting [11] and (3) melt mixing, with [15] and without [12,13] surface treatments. For the case of polymer blends, nanotubes offer a promising alternative to spherical particles and fibers commonly used as additives in polymer blends because of their large surface-to-volume ratio and structural anisotropy as well as the chemical moieties that may be grafted to their surfaces. WS<sub>2</sub> nanotubes were chosen as additives because a suitable scheme for chemical functionalization and dispersion into the PS/PMMA matrix could be found (see below).

The choice of the PS/PMMA polymer blend system was motivated by the fact that the bulk and surface properties of both homopolymers are well-known as well as PS–PMMA interactions such as interfacial tension [16], the Flory interaction parameter [17] vs. temperature and the individual surface tensions [18]. Reference data for unfilled blends has previously been reported [19–21]. From the point of view of preparation and characterization, the PS/PMMA system has several advantages. Both polymers and appropriately functionalized nanotubes may be mixed in toluene and the resulting solutions used for spin-casting thin films. Conveniently, differential solvents exist for the PS/PMMA combination (for example, cyclohexane dissolves PS but not PMMA while acetonitrile dissolves PMMA but not PS), which allows selective removal of one component and subsequent imaging by atomic force microscopy (AFM) of the remaining polymer. The PS/PMMA pair also has good X-ray adsorption contrast near the carbon absorption edge [22], due to presence of oxygen in PMMA only, allowing us to obtain chemically-specific images with scanning transmission X-ray microscopy (STXM, Ref. [23]). Finally, the high-Z WS<sub>2</sub> may be imaged in the polymer matrix by transmission electron microscopy (TEM).

## 2. Experimental section

*Preparation of PS/PMMA/WS<sub>2</sub>.* Nanocomposites (NC) required functionalization of the multiwall WS<sub>2</sub> nanotubes.

Mixing of non-functionalized nanotubes in a common solvent for PS and PMMA resulted in phase separation of the nanotubes into a precipitate separate from both the solvent and the polymers. Initial attempts to functionalize the nanotubes in solutions of surfactants were not successful. On the other hand, sonication in toluene in the presence of the surfactant, *n*-octadecyl phosphonic acid (OPA, C<sub>18</sub>H<sub>37</sub>PO<sub>3</sub>H<sub>2</sub>), was facile and effective, binding the PO<sub>3</sub>H<sub>2</sub> head group to the surface of the nanotubes. Similar results have been reported for the binding of phosphonic acid to powdered ZrO<sub>2</sub>, TiO<sub>2</sub> and zirconated silica by Gao et al. [24], using a solution reaction (without sonication). The coating of WS<sub>2</sub> was achieved by ultrasonic irradiation of a slurry of nanotubes in OPA with a WS<sub>2</sub>–acid ratio of 10:1 (by weight) in 50 ml toluene, under air atmosphere at 273 K, using a high-intensity ultrasonic probe (Sonics Vibra cell VC-601, 13 mm Ti horn, operated at 20 kHz with intensity 100 W/cm<sup>2</sup>). The mixture was sonicated for 2 h, followed by at least 5 cycles of centrifuging and washing in toluene to remove any unreacted acid. The product was then dried in vacuum.

*Preparation of nanotubes–polymer blends.* The functionalized nanotubes were mixed with toluene containing PS and PMMA and spun-cast onto polished silicon or Si<sub>3</sub>N<sub>4</sub> (for the STXM experiments, see below) substrates to produce thin films of the blend nanocomposites. We note that the tail groups on the nanotubes have weakly unfavorable chemical interactions with both polymers (though less so with PS than PMMA), the main purpose of the coating in this case being the prevention of particle agglomeration. The small size of the coated nanoparticles enables them to remain dispersed within the blend. (Future work will involve the use of pyridine or propylene oxide functional groups attached to the ends of the adsorbed chains, having favorable interactions with PMMA and PS, respectively).

*FTIR spectra.* Fourier transform infrared (FTIR) spectra were collected on a Nicolet 760 Magna spectrophotometer equipped with a He–Ne laser and a MCT (mercury cadmium telluride, HgCdTe) detector. Spectral resolution was 2 cm<sup>−1</sup>.

*AFM experiments.* Samples for AFM imaging were prepared by spin-casting 100–120 nm layers onto flat, polished silicon wafers containing 0, 10 and 20% (by weight) nanotubes mixed in toluene with a 50/50 (by weight) PS (*M<sub>w</sub>* = 90 or 123K)/PMMA (*M<sub>w</sub>* = 35K) blend. The specimens were annealed at 170 °C (well above the glass transitions of both polymers of approximately 105 °C) in a vacuum oven for times of up to one week. AFM images were obtained with a Digital Instruments Dimension 3000 or Topometrix Explorer using Si<sub>3</sub>N<sub>4</sub> tips having nominal tip radii of 20 nm and stiffness of ~0.1 N/m. The AFM was operated in contact mode to record topographic and lateral force (friction) images.

*STXM experiments.* To further characterize the domain sizes and structures, we performed STXM experiments on

the nanocomposite films. This is a high-resolution technique [23] where a focused X-ray beam is used to image the polymers by measuring adsorption spectra near the carbon edge at 284.5 eV photon energy. Experiments were done on the STXM undulator beamline X1A of the National Synchrotron Light Source at Brookhaven. In this setup, X-rays from a spherical-grating monochromator (energy resolution 0.4 eV at 290 eV) are incident on a Fresnel zone plate, which focuses the beam onto the specimen with a spot size of 40 nm. Carbon adsorption spectra are measured in transmission over an energy range of 280–320 eV with a high rate gas proportional counter (90% Ar/10% CO<sub>2</sub> gas mixture). Chemical-specific images are obtained by translating the sample laterally with piezoelectric scanners and measuring the transmitted intensity at various fixed energies.

Since the STXM experiment is done in transmission, both the substrate and sample must be thin (less than  $\sim 100$  nm each) to have adequate transmitted intensity. Si<sub>3</sub>N<sub>4</sub> membranes, 100 nm thick and suspended within a 0.5 mm square frame, were used as substrates. Thin-film samples of the nanocomposite could be spun-cast onto these substrates just as for the thicker silicon substrates used for AFM experiments.

### 3. Results and discussion

Fig. 1 shows FTIR spectra for the uncoated WS<sub>2</sub> nanotubes, pure OPA, and OPA-coated nanotubes. The characteristic methylene group asymmetric ( $\nu_{as}$  CH<sub>2</sub>, 2917 cm<sup>-1</sup>) and symmetric ( $\nu_s$  CH<sub>2</sub>, 2850 cm<sup>-1</sup>) stretching vibrations [25] appear in the OPA-WS<sub>2</sub> spectrum as broad bands, suggesting that the alkyl chains are not close packed. The region of the spectrum associated with P–O stretching vibrations (1300–800 cm<sup>-1</sup>) has previously been used to assess the binding of the phosphonate group to metal oxide surfaces [24]. The peak with overlapping vibrations at  $\sim 1240$  cm<sup>-1</sup> is identified as due to the P=O bond and several peaks around 1010 cm<sup>-1</sup> are identified as being derived from the P–O–H bond. In addition to some broadening of the peaks relative to pure OPA, there are

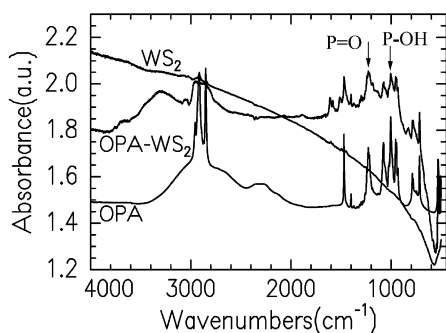


Fig. 1. FTIR absorption spectra for pure *n*-octadecyl phosphonic acid (OPA), OPA-coated WS<sub>2</sub> nanotubes and uncoated WS<sub>2</sub> nanotubes.

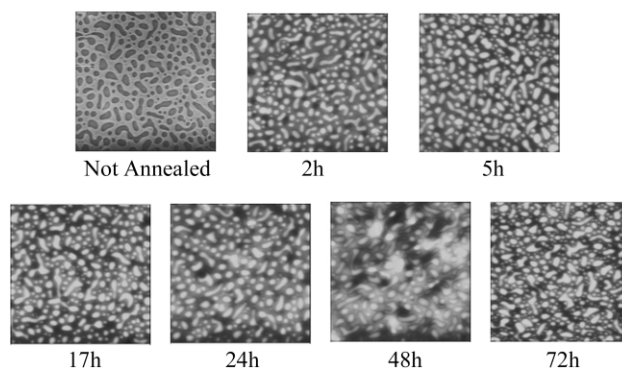


Fig. 2. AFM topographic scans, 20  $\mu\text{m} \times 20 \mu\text{m}$ , for 50/50 (by weight) PS(90 K)/PMMA(35 K) blends filled with 10 wt% OPA-WS<sub>2</sub> and annealed at 170 °C for times up to 72 h. Height scale is 110 nm, darker is deeper and lighter is higher.

new peaks at 1293 and 830 cm<sup>-1</sup> in the spectrum for the coated nanotubes. It is likely that the bonding of the phosphonate group to the WS<sub>2</sub> nanoparticle surface is not unique.

Figs. 2 and 3 show a series of AFM topography scans, 20  $\mu\text{m} \times 20 \mu\text{m}$  scan width, for PS/PMMA blends with and without addition of 10 wt% OPA-coated WS<sub>2</sub> nanotubes, respectively, which were annealed at 170 °C for times up to 72 h. The blend without filler (Fig. 3) shows, as previously observed [20], the development of large phase-separated circular droplets of PS, diameter  $\approx 5 \mu\text{m}$ , on top of an adsorbed PMMA layer, characteristic of the highly immiscible pure PS/PMMA blend. The filled blend series, Fig. 2, shows the phase separation process essentially frozen-in after 2 h, with smaller,  $\approx 1 \mu\text{m}$ , irregularly shaped domains and a considerably reduced surface roughness of 10–12 nm (vs. 130 nm for the 72 h annealed blend sample without nanotubes, see Fig. 4). In this case we may be seeing the beginning stages of the transition to a rod-induced morphology predicted by the simulations of Peng et al. [26].

The X-ray absorption spectra for pure PS and PMMA are shown in Fig. 5, where it can be seen that for a photon energy of 285.3 eV (corresponding to the C<sub>1s</sub>  $\rightarrow \pi_{C=C}^*$  transition) nearly all of the absorption is due to PS, while at 288.6 eV (corresponding to the C<sub>1s</sub>  $\rightarrow \pi_{C=O}^*$  transition) most of the absorption is due to PMMA, with the area ratio of the

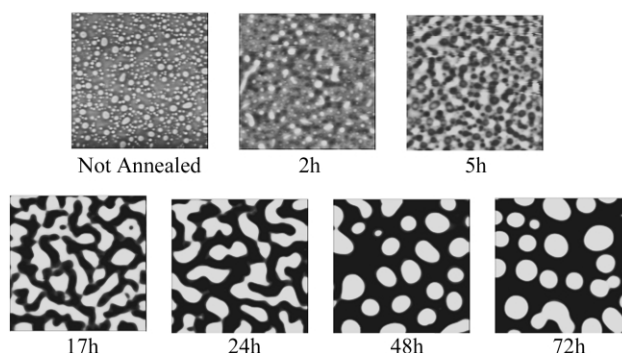


Fig. 3. As Fig. 2, but without nanotube fillers added. All scales are same as Fig. 2.



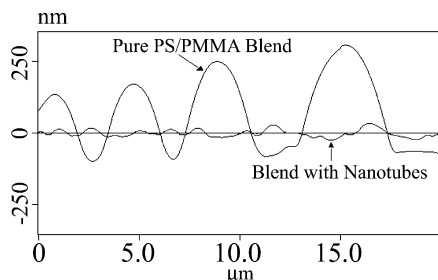


Fig. 4. Surface height scans for the 72 h anneal samples of Figs. 2 and 3.

respective peaks  $A_{\text{PMMA}}/A_{\text{PS}} = 12.5/5$ . Therefore images were made at these two energies to record 'PS' and 'PMMA' images. Scans were also taken at approximately 316 eV, where the fact that PS and PMMA absorption rates are similar makes the image mostly sensitive to the total sample thickness and can be used to monitor uniformity of sample thickness.

Fig. 6(a) and (b) show  $20\ \mu\text{m} \times 20\ \mu\text{m}$  PS and PMMA images, respectively, of a 100 nm film containing 10 wt% nanotubes annealed for 24 h at 170 °C. In the micrographs, darker areas represent greater absorption, hence greater thickness, for PS (Fig. 6(a)) and PMMA (Fig. 6(b)). The images show PMMA domains of linear dimensions 0.5–1  $\mu\text{m}$  across, of irregular shape, likely reflecting the presence of the nanotubes at the PS–PMMA interfaces, surrounded by a connected PS matrix. In Fig. 7(b) and (c) are shown two absorption vs. energy spectra for the corresponding locations in the PMMA-rich and PS-rich domains of the image in Fig. 7(a). Comparison with the absorption spectra for pure PS and PMMA of Fig. 5 indicates that the domains are nearly pure, estimated to be >90% PMMA in (1) and PS in (2). The STXM measurement represents an integral absorption coefficient along the path of the X-ray beam, normal to the sample surface, so the above implies vertically oriented domains relative to the substrate.

Further insight into the structure of the domains may be obtained by 'washing' away one of the phases in a differential solvent [27]. Fig. 8 shows an AFM image and sectional line-scan for a filled blend sample washed in

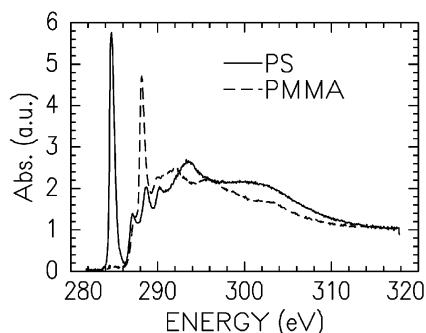
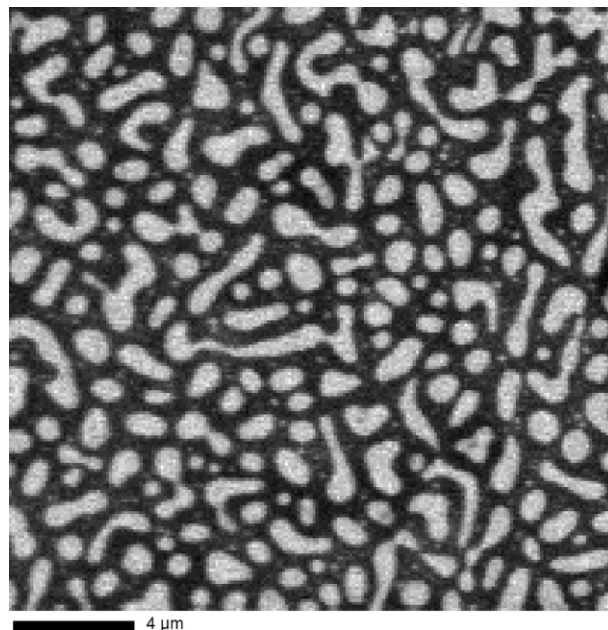
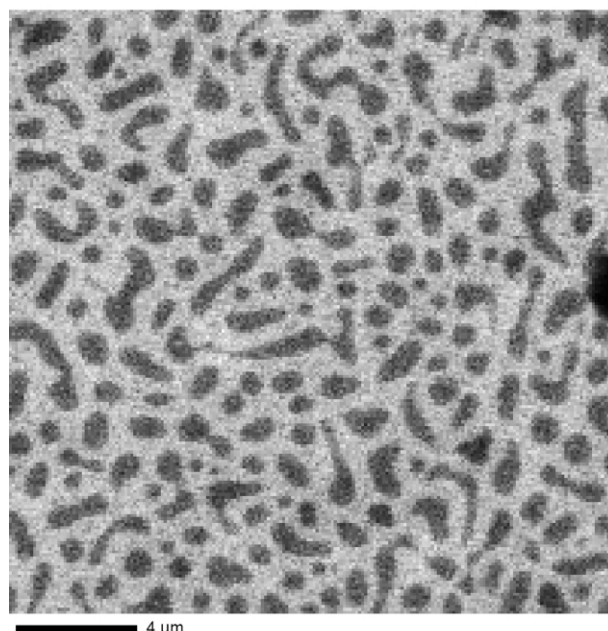


Fig. 5. X-ray absorption spectra near the carbon edge for pure PS and PMMA samples. Absorbance is in arbitrary units (au).



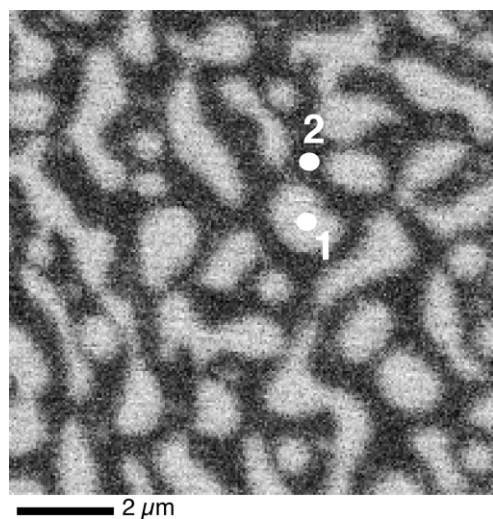
(a)



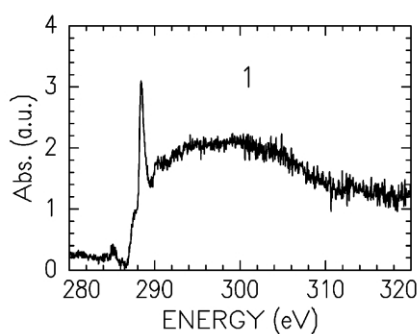
(b)

Fig. 6. Scanning transmission X-ray absorption microscopy (STXM) images for 50/50 (by weight) PS (123 K)/PMMA (35 K) blends with 10 wt% OPA-WS<sub>2</sub> fillers, annealed 24 h at 170 °C, (a)  $E_{\text{X-rays}} = 285.3\ \text{eV}$ , (b)  $E_{\text{X-rays}} = 288.6\ \text{eV}$ . Darker regions indicate greater absorption, hence greater thickness, for PS (a) or PMMA (b).

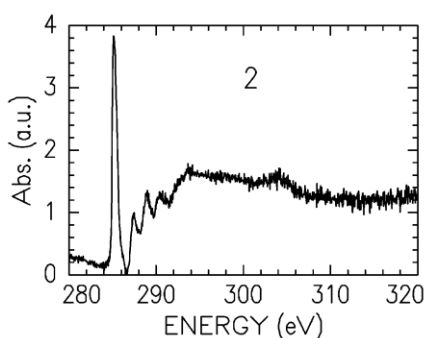
cyclohexane, a good solvent for PS and a non-solvent for PMMA. The depth of the contours in the AFM image of the remaining PMMA is consistent with a thin wetting layer of PMMA preferentially adsorbed at the silicon oxide-covered substrate, similar to the behavior of pure PS/PMMA blends [20]. Since the surface tension of PS is less than that of



(a)



(b)



(c)

Fig. 7. (a) STXM image for  $E_{X\text{-rays}} = 285.3$  eV (darker = PS regions), (b), (c) absorption scans for locations marked 1 and 2 in (a). Sample as in Fig. 6 except annealed 5 h at 170 °C.

PMMA, it is also possible that a thin PS layer covers the PMMA domains, though we cannot confirm or rule this out from our data.

Finally, we address the issue of the nanoparticle dispersion in the blend. TEM was used to image individual nanotubes (Fig. 9(a) and (b)). Samples were prepared by removing the thin films from the silicon substrates using an aqueous KOH solution, which attacks the silicon oxide

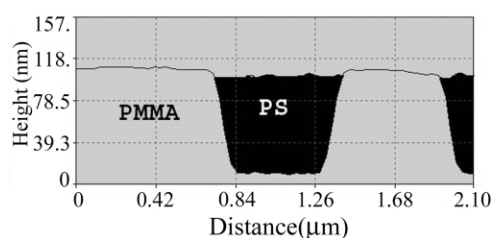
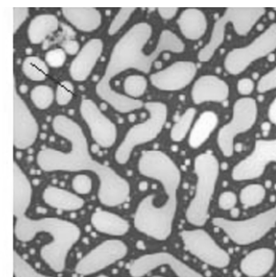


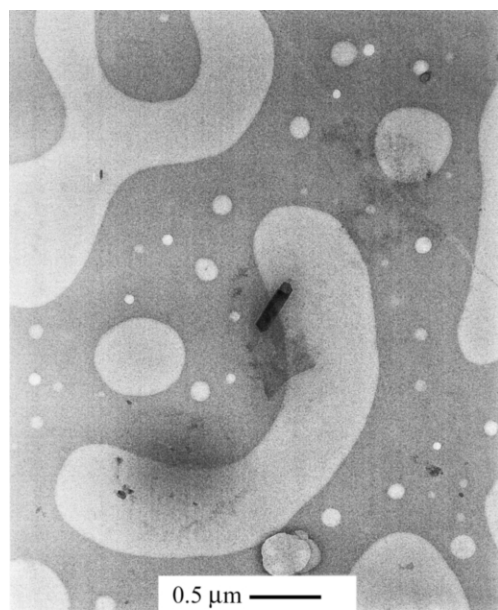
Fig. 8. AFM topographic image (top), 10  $\mu\text{m} \times 10 \mu\text{m}$ , and line scan (bottom) for sample washed in cyclohexane (to dissolve PS). Sample as in Fig. 6. Height scale for image is 157 nm, darker is deeper and lighter is higher.

layer, and floating onto a standard 3 mm diameter copper TEM grid. The nanotubes were not found to preferentially segregate to either the PS or PMMA phases. The lengths of the tubes were typically 200–500 nm, far less than their original size of 10–20  $\mu\text{m}$ , presumably due to the effects of sonication and spin casting.

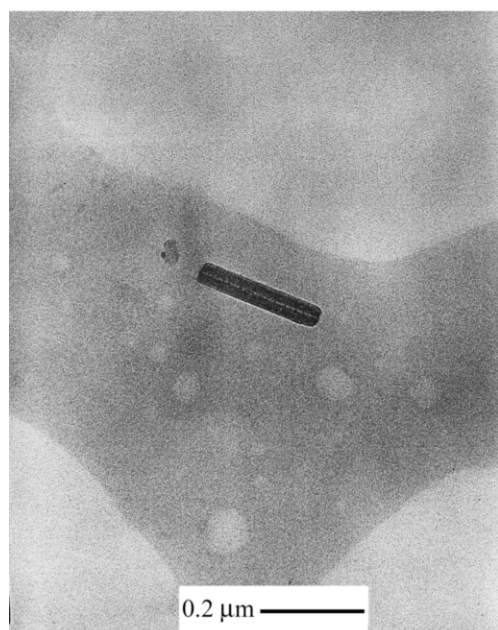
The presence of the nanotubes can also be observed, though less directly, with atomic force microscopy (AFM). Fig. 10 shows topographic and friction force AFM images for a 24 h annealed sample. No obvious structures due to the nanotubes are visible in the topography, indicating that the nanotubes are not segregated to the free surface. The friction force image clearly shows dark spots (corresponding to lower friction) associated with the nanotubes. No friction images of the PS/PMMA blends without nanotubes showed these features. As can be seen, the nanotubes are well dispersed, although a slight tendency of tubes to align along the interfaces between PS and PMMA is evident.

#### 4. Conclusions

We have found an efficient method of functionalizing  $\text{WS}_2$  nanotube particles using sonication in toluene to produce nanotubes coated with octadecyl phosphonic acid. The coated particles could then be mixed into the PS/PMMA polymer blend to create new nanocomposite materials. In thin films, the resulting mixtures were found to have dramatically reduced domain size and surface roughness. The nanotubes were observed to be dispersed into both PS and PMMA phases, though we



(a)



(b)

Fig. 9. Transmission electron microscopy (TEM) images of isolated OPA-WS<sub>2</sub> nanotubes in filled blend. Sample as in Fig. 6.

cannot exclude the possibility that at equilibrium (which apparently would take much longer to reach than the time scale of our experiments) there could be segregation to one phase. We believe that the ‘freezing-in’ of the process of phase separation (Fig. 2) is due to the large volume of material effectively immobilized by proximity to the nanoparticles, similar to observations on other filled systems with large surface/volume ratios

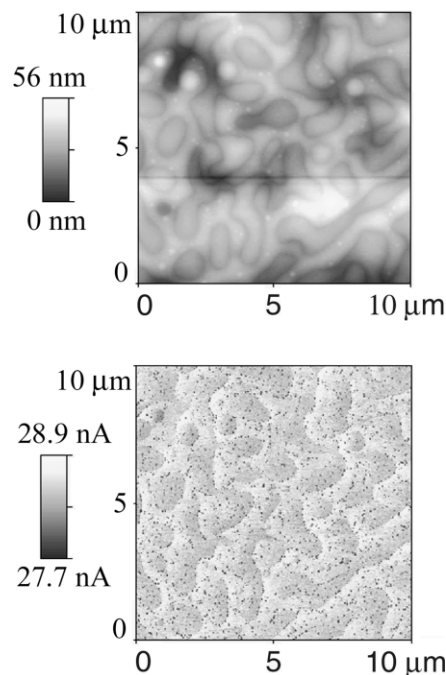


Fig. 10. AFM topographic (top) and friction (bottom) images for sample as in Fig. 6.

[3,5]. Further work to optimize blend properties as a function of nanotube size and coating functionality is in progress.

### Acknowledgements

This work is supported by the NSF under the MRSEC program (DMR-9632525, Stony Brook, Polytechnic, NC State) and NSF grant DMR-007143 (NC State) and at the Weizmann Institute under the Israeli Ministry of Science ‘Tashtiot’ program. J.S. gratefully acknowledges the support of the Joseph Meyerhoff Visiting Professorship at the Weizmann Institute.

### References

- [1] For a review, see Di Lorenzo ML, Frigione M. *J Polym Engng* 1997; 17:429–59.
- [2] Pukánszky B, Fekete E. In: Jancar J, editor. *Adhesion and surface modification. Advances in polymer science*, vol. 139. Berlin: Springer; 1999. p. 109.
- [3] Hornsby PR, Mthupa A. *J Mater Sci* 1994;29:5293–301.
- [4] Suetsugu Y, White JL. *J Appl Polym Sci* 1983;28:1481–501.
- [5] Nesterov AE, Lipatov YuS, Horichko VV, Gritsenko OT. *Polymer* 1992;33(3):619–22. and references therein.
- [6] Tenne R, Margulis L, Genut M, Hodes G. *Nature* 1992;360:444–6.
- [7] Rapoport L, Bilik Yu, Feldman Y, Homyonfer CSR, Tenne R. *Nature* 1997;387:791–3.
- [8] Rothschild A, Sloan J, Tenne R. *J Am Chem Soc* 2000;122:5169–79.
- [9] Iijima S. *Nature* 1991;354:56–8.
- [10] Shaffer MSP, Windle AH. *Adv Mater* 1999;11:937–41.

- [11] Stephan C, Nguyen TP, de la Chapelle ML, Lefrant S, Journet C, Bernier P. *Synth Mater* 2000;108:139–49.
- [12] Jin Z, Pramoda KP, Xu G, Goh SH. *Chem Phys Lett* 2001;337:43–7.
- [13] Andrews R, Jacques D, Minot M, Rantell T. *Macromol Mater Engng* 2002;287:395–403.
- [14] Velasco-Santos C, Martinez-Hernandez AL, Lozado-Cassou M, Alvarez-Castillo A, Castano VM. *Nanotechnology* 2002;13:495–8.
- [15] Jin Z, Pramoda KP, Goh SH, Xu G. *Mater Res Bull* 2002;37:271–8.
- [16] Anastasiadis SH, Gancarz I, Koberstein JT. *Macromolecules* 1988;21:2980–7.
- [17] Russell TP, Hjelm RP, Seeger PA. *Macromolecules* 1990;23(3):890–3.
- [18] Sauer BB, private communication.
- [19] Tanaka K, Takahara A, Kajiyama T. *Macromolecules* 1996;29:3232–9.
- [20] Walheim S, Boltau M, Mlynek J, Krausch G, Steiner U. *Macromolecules* 1997;30:4995–5003.
- [21] Ton-That C, Shard AG, Teare DOH, Bradley RH. *Polymer* 2001;42:1121–9.
- [22] Ade H, Zhang X, Cameron S, Costello C, Kirz J, Williams S. *Science* 1992;258:972–5.
- [23] Jacobsen C, Williams S, Anderson E, Browne MT, Buckley CJ, Kern D, Kirz J, Rivers M, Zhang X. *Opt Commun* 1991;86:351–64.
- [24] Gao W, Dickinson L, Grozinger C, Morin FG, Reven L. *Langmuir* 1996;12:6429–35.
- [25] Gatin M, Anderson MR. *Vibr Spectrosc* 1993;5:255–61.
- [26] Peng G, Qiu F, Ginzburg VV, Jasnow D, Balazs AC. *Science* 2000;288:1802–4.
- [27] Lambooy P, Phelan KC, Haugg O, Krausch G. *Phys Rev Lett* 1996;76:1110–3.